A MULTIRESOLUTION APPROACH TO FLOW FEATURE EXTRACTION FROM PHASE CONTRAST MAGNETIC RESONANCE ANGIOGRAPHY

A H Bhalerao and P E Summers [1]

Introduction

Magnetic resonance imaging (MRI) is used to map the distribution and dynamics of nuclei such as hydrogen. Imaging can be adapted to show blood in contrast to the surrounding sationary tissues. This application of MRI referred to as MR angiography (MRA) has become widely used in cardiovascular assessment because of its sensitivity to disease states and lack of ionising radiation or iodinated contrast agent. The two main classes of MRA techniques use blood's motion to modify the intensity (Time of Flight techniques) or phase (Phase Contrast techniques) of the blood signal relative to that of static tissues. Time of Flight techniques are most widely available, but have severe limitations in terms of robustness of the quantifiable relationship. Phase constrast angiography (PCA) produces a vector image i.e. estimates are formed of three orthogonal components of the velocity field. In effect, not one, but four images are obtained - a T1-weighted anatomical image, and three images of orthogonal velocity components.

Phase-contrast magnetic resonance angiography provides a uniquely rich information content in a relatively short imaging time. Typically only the intensity (representing the speed of flow) is displayed in clinical images as *maximum intensity projections* (MIP). The information, therefore, is only crudely communicated and, in particular, directionality and magnitude of velocity are not conveyed to the viewer. Similarly, surface rendered views of the vessel represent only a thresholding of the net velocity and require the user to interactively minimise the number of disjoint structures. To incorporate the function information into an image which also portrays the spatial arrangement of vessels is a difficult task, with the large volumes of data which may be present. Much of the post-processing of MRA data is aimed at better visualisation - (e.g. MIP), particularly image enhancement, such as improving contrast and local connectivity [1], or reducing flow artifacts to better determine blood flow streamlines [2]. These workers have employed iterative, local optimisation methods to improve flow estimates by essentially smoothing the data constrained by anatomical structure. Relatively little work has been done in using more sophisticated techniques currently being used by researchers in computer vision.

This paper considers the automatic extraction of a concise symbolic representation of vasculature [3]. The model-based approach makes direct use of the vector magnitude and direction information to form velocity averages over a succession of scales. The resulting oct-tree representation in turn is well suited to further extensions and manipulations for display and processing of the data. Moreover, the data volume is reduced in accordance with the sparsity of the vascular network making subsequent manipulations more efficient than is possible when handling the full data volume.

A Multiresolution Model for Curves in 3D

The model used here for the segmentation of MRA data is an extension to 3D of the simple 2D curve segmentation model used by Calway [4] and is based on a general class of linear multiresolution image

[1] A H Bhalerao and P E Summers are with the Departments of Medical Physics and Radiological Sciences, Guy's and St. Thomas' Hospitals and UMDS, London

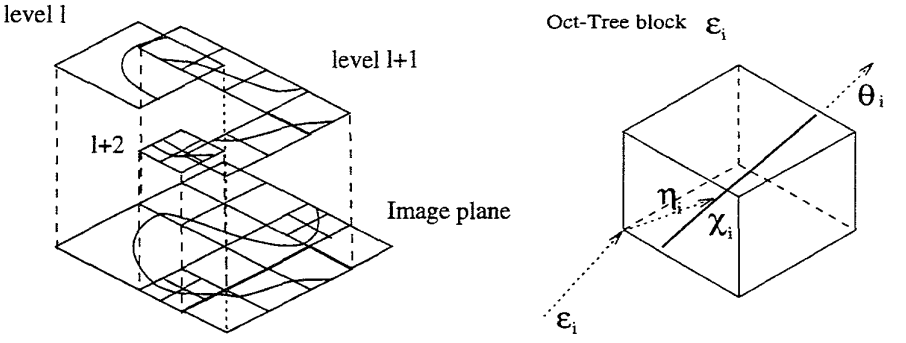

(a) A multiresolution image model for curves (b) Curve tangent estimate

Figure 1: Curve Model

models [5]. The generalised linear multiresolution image model may be defined by a recursive operation:

$$s_{ijk}(l) = \sum_{mno} A_{ijk,mno}(l) s_{mno}(l-1) + \sum_{pqr} B_{ijk,pqr}(l) w_{pqr}(l) \tag{1}$$

where $s_{ijk}(l)$ is the 'image' at level l of the model given by taking a *linear* combination of the level above (*lower* spatial resolution) plus an *innovations* image $w_{pqr}(l)$. The linear operators A and B 'construct' the image by controlling the features from the coarser, 'parent' resolution and the innovations used to form the 'child' level. The resulting image $s_{ijk}(M)$ is given by level M of the model. Figure 1(a) illustrates a typical realisation of the 2D model for a curve network. Local image features are represented at different scales, creating an inhomogeneous *tessellation* of the image into square regions (blocks) of different sizes. The larger features are represented by larger blocks at coarser spatial resolutions whereas detail, e.g. high curvature, is represented by smaller blocks. Each of these regions is subjected to the constraint of containing a *single* local feature.

The curve model is particularly simple to generate as these linear operators act as selection functions taking an appropriate octant of the previous level or of the innovation level. Each block is a locally defined real function which has an associated orientation and position vector, which models a single line feature in each block (*prototype*)[4] . The prototype can be extended to model both region and boundary features, including corner and branch points [6].

Segmentation

Within the framework of the 3D model, the segmentation process amounts to estimation of its parameters with decisions based on scale consistency criteria, whose aim is to tessellate the *phase-space* (oct-tree) into the smallest set of disjoint regions for which the data are consistent with the model. The best-fit tessellation is then transformed into a *Boundary Adjacency Graph* which is a symbolic representation of the feature blocks and their neighbourhood relationships. From this 3D curves, representing the vessel centre lines, are inferred by a relaxation process. Because of the great data reduction achieved by this stage, it is possible to use exhaustive graph-theoretic methods without the fear of exponential computation burden.

1. Oct-tree generation

The first step is to generate an oct-tree of the PCA data which is a volume of flow vectors $\mathbf{x}_{ijk}, 0 \leq i,j,k < N = 2^M$. The general form of processing is:

$$\mathbf{x}_{ijk}(l) = \sum_{m=-K}^{K} \sum_{n=-K}^{K} \sum_{o=-K}^{K} A_{mno} \mathbf{x}_{(2i-m)(2j-n)(2k-o)}(l+1) \tag{2}$$

where there are $M+1$ levels, $0 \leq l \leq M$, and the base of the oct-tree is the image $\mathbf{x}_{ijl}(M) = \mathbf{x}_{ijl}$ and the generating kernel A_{mno} is of size $(2K+1) \times (2K+1) \times (2K+1)$. Note that the scale index l appears as the argument of the function $\mathbf{x}(l)$, whereas the spatial indices are given as the subscripts $\mathbf{x}_{ijk}$. In the following, each oct-tree node $x_{ijk}(l)$ is denoted by the scale-space position vector $\vec{\xi}(l) = (i,j,k,l)^T$ and represents a cubic voxel region $\Lambda_{\vec{\xi}}$ of the image volume (at level M).

2. Tessellation

Starting at the coarsest spatial resolution, the oct-tree is traversed in a *pre-order* traversal (root, followed by sub-trees), and terminated if the highest spatial resolution is reached. A decision is taken at each node $\vec{\xi}$ to either terminate the tree at this point or to continue the search to the next, higher resolution:

$$\begin{aligned} \text{Hypothesis} \quad & H_0: \quad \text{there is no feature or a single feature in block} \\ \text{Accept} \quad & H_0 \quad \text{if } c_{\vec{\xi}} < T_n \text{ or } c_{\vec{\xi}} > T_c \end{aligned} \tag{3}$$

where c measures the coherence of the flow vectors within the block and is calculated by

$$c_{\vec{\xi}} = \frac{|\sum_{ijk \in \Lambda_{\vec{\xi}}} \mathbf{x}_{ijk}|}{\sum_{ijk \in \Lambda_{\vec{\xi}}} |\mathbf{x}_{ijk}|} \tag{4}$$

which is simply the 'length of the average flow vector' over the 'average length'. This measure has the characteristic of being small if the vectors are randomly oriented, i.e. they sum to zero, and large if there is a strongly oriented feature in the given block. The significance threshold T_n is set low to exclude noisy blocks where there is little or no coherent signal activity, and T_c set high to include only highly consistent blocks. An important property of this approach is the that the hypothesis testing may be repeated with lowered significance levels when there is sufficient evidence of a feature in a given locality. This can be used to good effect to close gaps in detected curve segments by re-examining the raw data (see below).

A Hough Transform [7](HT) is used in each trace point block to determine the feauture position $\vec{\eta}_m$ given that the orientation or slope $\vec{\theta}_m$ is already known. The resulting parameters of each trace point block are $\phi_i(l) = \{\vec{\xi}_i(l), \vec{\eta}_i(l), \vec{\theta}_i(l)\}$ (figure 1(b)).

3. Curve Inference and Tracing

The oct-tree nodes selected from the tessellation process are linked together to form an Adjacency Graph [8]. Nodes are considered neighbours if they either share a face, an edge or a vertex, or a combination of these attributes. In a homogeneous 3D grid, a node would have altogether 26 possible neighbours: 6 face, 12 edge and 8 vertex.

Each link $\lambda_{ij}(l,m)$ between neighbouring blocks (i,j) is given a strength based on the direction of the link, given by the angle of the displacement vector $\vec{\gamma}_{ij} = \vec{\chi}_i - \vec{\chi}_j$, and the orientation (slope) of the feature estimates of the blocks it connects:

$$P(\lambda_{ij}(l,m)|\phi_i(l), \phi_j(m)) = f_1(\theta_i(l) - \angle\vec{\gamma}_{ij}(l,m)) \times f_1(\theta_j(m) - \angle\vec{\gamma}_{ij}(l,m)) \tag{5}$$

and $f_1(\theta) = 0.5(1 - \cos\theta)$ which is at a maximum at $\theta = \pm\pi$.

All possible pairs of links from each node are ordered into decreasing likelihood that they locally form a curve segment. For a node with n links, there are a possible $n(n-1)/2$ link pair combinations. Each pair combination is given a probability defined to be

$$P(\lambda\lambda_x) = P(\vec{\gamma}_{x0})P(\vec{\gamma}_{x1})f_3(\angle\vec{\gamma}_{x0}, \angle\vec{\gamma}_{x1}) \tag{6}$$

where the subscripts $x0$ and $x1$ refer to the first and second links of the link pair set. The function $f_3(\theta) = 0.5(1 - \cos\theta)$, which has maxima at $\theta = \pm\pi$, expresses the requirement to give the highest probability to the 3-block curve segment with the minimum curvature.

Next, starting from the largest spatial blocks where the feature estimate is likely to be most reliable, curves are traced in both directions. The curve is continued by selecting a link λ_{ij} if the link is a member of the maximum probability pair in both blocks it connects. Curves with greater curvature segments can be included by relaxing this condition to allow for linking through link pairs which have lower probabilities. If a curve cannot be traced further within the continuation criteria, it is terminated and a new curve begun. Traced curves are not allowed to visit a given block more than once in an attempt to find as many independent paths through the trace points as possible. Thus far, no attempt has been made to join these extracted curve segments with each other using a higher-order process.

It has been already been demonstrated in [4] [9] etc. that within such a scheme, it is possible to fill gaps where there is *no* feature estimate and span more than a 1st order neighbourhood within the adjacency graph, by re-examining the original data in light of the greater confidence gained from results of the initial segmentation. Also, the sparseness of the symbolic structure obtained by this stage permits iterative schemes to be used, which would otherwise be computationally prohibitive [6].

Results

Figures 2(a)-(d) illustrate stages of the multiresolution curve-extraction algorithm run on part of a MRA of the head. The original data set was $256 \times 256 \times 64$ and the figures illustrate one 64^3 part of this data set. The surface rendered view in figure 2(a) is provided for comparison.

The result of the initial segmentation where the data set is tessellated into voxel blocks is shown in figure 2(b). The larger voxel blocks originate from coarser resolutions of the oct-tree expansion of the original data, whereas the smaller blocks have been chosen from the finer spatial resolutions. The single feature criterion tested by the hypothesis of equation (3) results in relatively large features being represented at the coarser resolutions and the finer detail and high curvature at the higher spatial resolutions. The background area of the image are areas of no significant activity (or noise blocks) and will be dead-branches in the octree. Each of the feature voxel blocks will equate to a trace point in the remainder of the algorithm. Figure 2(c) shows estimates of the slope of the features within each selected block, with each feature having a position offset within the block from the HT stage. The result of the curve tracking is shown in figure 2(d). Overall, there is good structural correspondence between the vessels seen in the voxel surface rendering and the extracted curves. In particular, local connectivity is established by the curve extraction in instances where there is fragmentation of the surface rendered view.

Conclusions

This paper has considered a multi-resolution, model based segmentation method for MRA. It is a spatial domain based technique and an extension to 3D of a 2D curve segmentation method reported elsewhere (e.g. [9]). It was demonstrated to produce a concise symbolic description of the MRA data (in the form of vessel centre lines) and is efficient in its computational complexity being equivalent in processing to filtering by a $3 \times 3 \times 3$ kernel,

and based on a generalised and flexible image model which has great potential as a basis for both qualitative and quantitative assessment of MRA data.

The work and results presented thus far are preliminary and currently there are several areas where consolidation and enhancement is necessary. There is a need to assess the levels of noise in the data in situ (as in [6]), to better control the confidence levels used for the hypothesis testing. Curve tracing is currently done probabilistically based purely on the local curvature. By considering the physical measurements of the data being imaged, e.g. speed of blood and the vessel diameters, local connectivity could be established using a conservation of mass constraint. Also, there is need to explicitly defined bifurcations as part of the signal model. With regards to visualisation, some experimentation has already been carried out to represent flow direction and using the multiresolution vectors for genererating filtered MIPs and predicting probable flow. The segmentation is also being applied to the estimation of blood pressure gradients *in vivo* [10].

Acknowledgements

The authors wish to acknowledge the assistance of the radiological staff at the at both St. Thomas' and Guy's Hospitals, Dr. David Hawkes (Radiological Sciences, Guy's) and members of the Image Processing Group, UMDS at Guy's Hospital.

This work is supported by the Special Trustees of St. Thomas's Hospital Trust.

References

1. W. A. Hanson D. Saloner and J. S. Tsuruda et al. Application of a Connected-Voxel Algorithm to MR Angiographic Data. *Journal of Magnetic Resonance Imaging*, 1:423–430, 1991.

2. M. H. Buonocore. Algorithms for Improving Calculated Streamlines in 3-D Phase Contrast Angiography. *Magnetic Resonance In Medicine*, 3(1):22–30, 1994.

3. G. Gerig, Th. Koller, G. Székely, Ch. Brechbühler and O. Kübler. Symbolic Description of 3-D Structures Applied to Cerebral Vessel Tree Obtained from MR Angiography Volume Data. In H. H. Barret and A. F. Gmitro (Eds.), editors, *Lecture Notes in Computer Science, N0. 687, Information Processing In Medical Imaging IPMI'93*, pages 94–111. Springer Verlag, 1993.

4. A. Calway and R. Wilson. Curve Extraction In Images Using the Multiresolution Fourier Transform. In *Proc. IEEE Conf. Acoust., Speech, and Signal Processing*, pages 2129–2132. IEEE, 1990.

5. S. C. Clippingdale and R. Wilson. Quad-Tree Image Estimation: A New Image Model and its Application to MMSE Image Restoration. In *Proc. 5th Scandinavian Conf. Image Analysis*, pages 699–706, Stockholm, Sweden, 1987.

6. A. Bhalerao and R. Wilson. Multiresolution Image Segmentation Combining Region and Boundary Information. In *Proc. 7th Scandinavian Conf. Im. Analysis*, pages 1162–1169, Aalborg, Denmark, 1991.

7. R. O. Duda and P. E. Hart. Use of the Hough Transform to Detect Lines and Curves in Pictures. *Communications of the ACM*, 15:11–15, 1972.

8. A. Bhalerao and P. Summers. Visualisation and Segmentation of 3D Phase Contrast Angiography Images. Technical report, Department of Medical Physics, St. Thomas' Hospital, London SE1 7EH, July 1994.

9. R. Wilson, A. D. Calway, and E. R. S. Pearson. A Generalized Wavelet Transform for Fourier Analysis: the Multiresolution Fourier Transform and its Application to Image and Audio Signal Analysis. *IEEE Trans. IT, Special Issue on Wavelet Representations*, 38:674–690, 1992.

10. P. E. Summers and A. H. Bhalerao. Derivation of Pressure Gradients from Magnetic Resonance Angiography Using Multi-Resolution Segmentation. In *Proc. IEE Conf. Image Processing and its Applications*, page in press, Edinburgh, U.K, 1995.

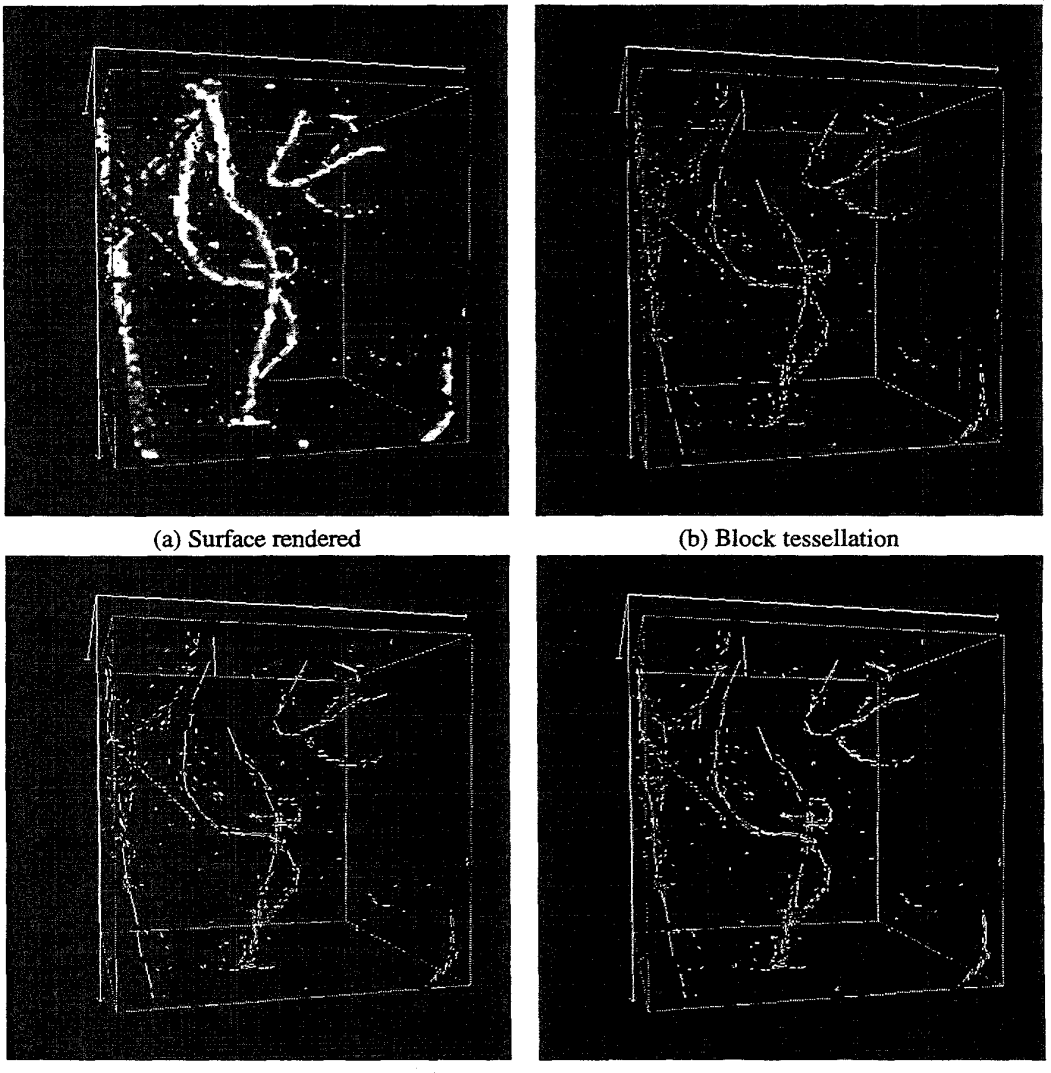

(a) Surface rendered (b) Block tessellation

(c) Curve features (d) Extracted curves

Figure 2: Results on one part of head data set